DALTON
FULL PAPER

# Silver(I) nitrate adducts with bidentate 2-, 3- and 4-pyridyl phosphines. Solution $^{31}P$ and [$^{31}P$–$^{109}Ag$] NMR studies of 1:2 complexes and crystal structure of dimeric [{Ag(d2pype)(μ-d2pype)}$_2$]-[$NO_3$]$_2$·2$CH_2Cl_2$ [d2pype = 1,2-bis(di-2-pyridylphosphino)ethane]

**Susan J. Berners-Price,*,†,[a] Richard J. Bowen,[a] Peta J. Harvey,[a] Peter C. Healy[a] and George A. Koutsantonis[b]**

[a] *School of Science, Griffith University, Nathan, Brisbane, Queensland 4111, Australia*
[b] *Department of Chemistry, University of Western Australia, Nedlands, Western Australia 6907, Australia*

The 1:2 complexes of silver(I) nitrate with 1,2-bis(di-*n*-pyridylphosphino)ethane (d*n*pype) for *n* = 2, 3 and 4 have been synthesized and solution properties characterized by NMR spectroscopy, including variable-temperature one-dimensional $^{31}P$-{$^1H$}, two-dimensional [$^{31}P$–$^{31}P$] COSY and [$^{31}P$–$^{109}Ag$] HMQC NMR experiments. The 3-pyridyl (d3pype) and 4-pyridyl (d4pype) complexes exist as bis-chelated monomeric [Ag(d3pype)$_2$]$^+$ and [Ag(d4pype)$_2$]$^+$ while the 2-pyridyl (d2pype) complex forms an equilibrium mixture of monomeric [Ag(d2pype)$_2$]$^+$, dimeric [{Ag(d2pype)$_2$}$_2$]$^{2+}$ and trimeric [{Ag(d2pype)$_2$}$_3$]$^{3+}$ species in which the d2pype ligands co-ordinate in both bridging and chelated modes *via* the phosphorus atoms. The relative percentages of the species present are dependent on both temperature and solvent. Crystals of the 2-pyridyl complex obtained from $CH_2Cl_2$–$Et_2O$ solution have been shown by crystal structure determination to be the dimer [{Ag(d2pype)(μ-d2pype)}$_2$]-[$NO_3$]$_2$·2$CH_2Cl_2$. Each silver ion is co-ordinated by one chelated and two bridging d2pype ligands forming a ten-membered ring in a double boat conformation. The pyridyl nitrogen atoms do not co-ordinate to the silver. The differences in solution behaviour of the three systems and the potential significance of these complexes to the antitumour properties of chelated 1:2 silver(I) diphosphine complexes are discussed.

Like their gold(I) counterparts, certain bis-chelated 1:2 silver(I) diphosphine complexes of the type [Ag(P–P)$_2$]$NO_3$ [where P–P is $Ph_2P(CH_2)_2PPh_2$ (dppe), *cis*-$Ph_2PCH{=}CHPPh_2$ (dppey) or $Et_2P(CH_2)_2PEt_2$ (depe)] have been shown to exhibit antitumour activity against *i.p* P388 leukaemia in mice, as well as antifungal and modest antibacterial properties.[1,2] Although the mechanism for the cytotoxicity is not known, tumour cell mitochondria are likely targets for these large lipophilic cations[3,4] and indeed the complex [Ag(eppe)$_2$]$NO_3$ [where eppe is $Ph_2P(CH_2)_2PEt_2$] exhibits selective primary antimitochondrial activity in yeast.[5] However, a major difficulty in the clinical use of these compounds is that they target mitochondria in all cells, resulting in unacceptably high levels of toxicity. Studies of the antitumour activity of other large lipophilic cations, such as bis quaternary ammonium heterocycles[6] and trialkylphosphium salts,[7] have demonstrated a relationship between antitumour selectivity and lipophilic–hydrophilic balance and we have adopted the approach in our work on the antitumour properties of [M(P–P)$_2$]$^+$ cations, of replacing the phenyl substituents of the diphosphine with pyridyl substituents in order to vary the hydrophilic character of the complexes.[8] As part of this work we report here the synthesis and characterization, by variable-temperature $^{31}P$-{$^1H$}, two-dimensional [$^{31}P$–$^{31}P$] COSY and [$^{31}P$–$^{109}Ag$] HMQC NMR spectroscopy, of the solution properties of 1:2 complexes of silver(I) nitrate with the diphosphine ligands 1,2 bis(di-*n*-pyridylphosphino)ethane (d*n*pype) for *n* = 2, 3 or 4 together with a single-crystal structure determination of the dimeric complex [{Ag(d2pype)(μ-d2pype)}$_2$][$NO_3$]$_2$·2$CH_2Cl_2$. The results show the d3pype and d4pype complexes to exist in solution as monomeric bis-chelated [Ag(d3pype)$_2$]$^+$ and [Ag(d4pype)$_2$]$^+$, whereas the d2pype complex forms equilibrium mixtures of monomeric [Ag(d2pype)$_2$]$^+$, dimeric [{Ag(d2pype)$_2$}$_2$]$^{2+}$ and trimeric [{Ag(d2pype)$_2$}$_3$]$^{3+}$ in which the d2pype ligands co-ordinate in both bridging and chelated modes with the relative percentages of the species present dependent on temperature and solvent.

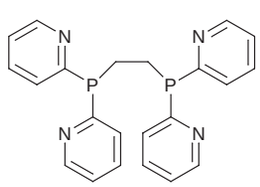

d2pype

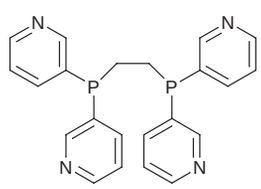

d3pype

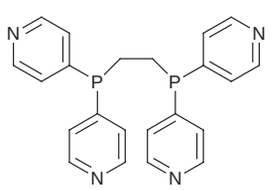

d4pype

## Experimental

### Preparation of compounds

The d*n*pype ligands for *n* = 2, 3 and 4 were prepared as described elsewhere.[9]

**[Ag(d2pype)$_2$]$NO_3$.** The compound $AgNO_3$ (0.077 g, 0.453 mmol) in water (1 cm$^3$) was added, with stirring, to a suspension of d2pype (0.4 g, 0.99 mmol) in acetone (20 cm$^3$) to give a

† E-Mail: S.Berners-Price@sct.gu.edu.au

clear solution. After further stirring for 1 h the solvent was allowed to evaporate at room temperature depositing white microcrystalline material (0.83 g, 94%), m.p. 277–287 °C (Found: C, 54.0; H, 4.5; N, 12.9; P, 12.6. $C_{44}H_{40}AgN_9O_3P_4$ requires C, 54.2; H, 4.1; N, 12.9; P, 12.7%). FAB mass spectrum: *m*/*z* 913 ($M^+$, 100%). ES mass spectrum: *m*/*z* 913, $[Ag(d2pype)_2]^+$; 1886 (1%), $[\{Ag(d2pype)_2\}_2^{2+} + NO_3^-]^+$. The material was readily soluble in polar organic solvents but only slightly soluble in water. Needle-like crystals of the solvated dimer, $\{[Ag(d2pype)_2]NO_3\}_2 \cdot 2CH_2Cl_2$, of marginal suitability for crystal structure determination, were obtained with considerable difficulty by vapour diffusion of $Et_2O$ into a $CH_2Cl_2$ solution of the complex.

**$[Ag(d3pype)_2]NO_3 \cdot 3H_2O$.** The compound $AgNO_3$ (0.061 g, 0.358 mmol) in water (0.4 $cm^3$) was added dropwise to a solution of d3pype (0.303 g, 0.75 mmol) in acetone (40 $cm^3$), resulting in the immediate formation of a fine white suspension. The volume of the solvent was concentrated to *ca*. 20 $cm^3$ and the flask cooled overnight at −20 °C. The cold suspension was filtered affording the complex as a microcrystalline solid (0.2 g, 57%), m.p. 230–235 °C (Found: C, 51.1; H, 4.4; N, 12.1. $C_{44}H_{46}AgN_9O_6P_4$ requires C, 51.4; H, 4.5; N, 12.3%).

**$[Ag(d4pype)_2]NO_3 \cdot 5H_2O$.** The compound $AgNO_3$ (0.084 g, 0.5 mmol) was added as a solid to a suspension of d4pype (0.4 g, 1.0 mmol) in tetrahydrofuran (20 $cm^3$). The mixture was stirred overnight and the resultant solid product collected by filtration. The solid was dissolved in methanol and insoluble material filtered off. The compound precipitated as a white solid on addition of $Et_2O$ to the filtrate (0.2 g, 41%), m.p. 225–233 °C (decomp.) (Found: C, 49.8; H, 4.5; N, 11.6. $C_{44}H_{50}AgN_9O_8P_4$ requires C, 49.7; H, 4.7; N, 11.9%).

Both the 3- and 4-pyridyl complexes were found to be highly soluble in water, dmso and methanol but insoluble in $CH_2Cl_2$. Despite many attempts, however, crystals of a size suitable for X-ray diffraction studies were not obtained for these two complexes.

### Spectroscopy

Electrospray (ES) mass spectra were recorded in acetonitrile solutions on a Quattro II mass spectrometer with a cone potential of 25 V, FAB mass spectra in a mixture of $CH_2Cl_2$ and *p*-nitrobenzyl alcohol on a VG Autospec mass spectrometer ($Cs^+$ ion gun) with an accelerating voltage of 8 kV.

Proton, $^{13}C$ and $^{31}P$ NMR spectra were recorded on either Varian Gemini-200 or UNITY-400 spectrometers and were referenced as indicated in Tables 1–3. Typically, $^{31}P$-$\{^1H\}$ spectra were recorded with a pulse angle of 45° and a relaxation delay of 2 s.‡ The $^{31}P$-$\{^{109}Ag\}$ NMR spectra were recorded on a Varian UNITY-400 spectrometer equipped with three RF channels and a 5 mm triple resonance $^{31}P[^1H/X]$ probehead with the X-channel tuned to $^{109}Ag$ at 18.64 MHz. The 90° pulse for $^{31}P$ was 12.3 μs and for $^{109}Ag$ 100 μs. Sample spinning was not used. Both one-dimensional $^{109}Ag$-edited $^{31}P$ spectra and two-dimensional $[^{31}P–^{109}Ag]$ spectra were recorded using an HMQC sequence. For $\{[Ag(d2pype)_2]NO_3\}_n$ $^1J(^{109}Ag–^{31}P)$ was optimized at 295 K for $n = 1$ (266 Hz) and at 243 K for $n = 2$ (310 Hz); WALTZ-16 modulated $^1H$ decoupling was applied throughout the whole sequence and the $^{109}Ag$ spins were not decoupled. Two-dimensional spectra were acquired using the Haberkorn–Ruben (hypercomplex) method for quadrature detection in F1. Typically, the spectral widths were 2000 and 5690 Hz in the F1 ($^{109}Ag$) and F2 ($^{31}P$) dimensions, respectively. Thirty-two time increments were used in each of which 32 to 160 transients were added, with a 1 s relaxation delay. The $^{31}P$ chemical shifts were referenced to external 85% $H_3PO_4$ (δ 0) measured at 295 K and the $^{109}Ag$ chemical shift reference was external 4 M $AgNO_3$ in $D_2O$. Two-dimensional phase-sensitive $^{31}P$ homonuclear shift correlated (COSY) spectra were recorded with WALTZ-16 modulated $^1H$ decoupling. The spectral width in F2 was 4068 Hz with 2048 data points. A total of 256 free induction decays were taken in F1 with 28 scans each. The recycle delay was set to 3 s to give a total experiment time of 14 h.

‡ These pulsing conditions allow a fairly accurate estimate of the relative concentrations of $[Ag(d2pype)_2]^+$ and $[\{Ag(d2pype)_2\}_2]^{2+}$ by comparison of peak integrals since their $^{31}P$ resonances have similar $T_1$ values: 1.71 ± 0.07 and 1.59 ± 0.03 s, respectively, as measured by the inversion recovery method for a solution of $\{[Ag(d2pype)_2]NO_3\}_n$ in $CD_3OD$ at 295 K.

### Crystallography

A unique room-temperature diffractometer data set (*T* 295 K; 2θ–θ scan mode, monochromatic Mo-Kα radiation, λ = 0.710 73 Å) was collected for $[\{Ag(d2pype)(\mu\text{-}d2pype)\}_2][NO_3]_2 \cdot 2CH_2Cl_2$ on a colourless crystal with dimensions 0.16 × 0.06 × 0.16 mm yielding 6080 independent reflections within the limit $2\theta_{max} = 45°$; 1438 of these with $I > 3\sigma(I)$ were considered 'observed' and used in the large-block least-squares refinement after Gaussian absorption correction ($A^*_{min,max} = 1.05, 1.12$). Crystals of the complex were of marginal quality and the quality of the resulting determination was correspondingly poor. The structure was solved by heavy atom Patterson methods, expanded using Fourier techniques and refined by full-matrix least squares on |*F*|. Limited data supported meaningful anisotropic thermal parameter refinement for Ag, P and $NO_3$ moieties only, all other atoms being modelled with the isotropic form. Hydrogen atoms were included with *x*, *y*, *z*, $U_{iso}$ constrained at estimated values. Difference map residues were modelled in terms of $CH_2Cl_2$ of solvation (chloride thermal parameters anisotropic). The N atoms of the 2-pyridyl rings were indistinguishable and modelled as disordered C, N composites over the pairs of possible sites. Conventional residuals *R*, *R′* at convergence were 0.078, 0.070 [statistical weights, derivative of $\sigma^2(I) = \sigma^2(I_{diff}) + 0.0004\sigma^4(I_{diff})$]. Neutral atom complex scattering factors were employed, computation using the XTAL 3.2 program, system implemented by S. R. Hall.[10]

**Crystal data.** $C_{90}H_{84}Ag_2Cl_4N_{18}O_6P_8$, *M* = 2119.2, monoclinic, space group $P2_1/c$ ($C^5_{2h}$, no. 14), *a* = 15.869(6), *b* = 18.315(8), *c* = 17.369(9) Å, β = 112.67(4)°, *U* = 4658 $Å^3$, $D_c$ (*Z* = 2 dimers) = 1.51 g $cm^{-3}$, *F*(000) = 2160, $\mu_{Mo}$ = 7.4 $cm^{-1}$.

CCDC reference number 186/940.

See http://www.rsc.org/suppdata/dt/1998/1743/ for crystallographic files in .cif format.

## Results and Discussion

In previous work we have investigated the solution structures of 1 : 2 adducts of $AgNO_3$ with the bidentate arylphosphines, dppe, dppp, *cis*-dppey, depe and eppe.[11,12] Solution $^{31}P$ NMR studies of these complexes showed evidence for only monomeric, bis-chelated ionic complexes of type $[Ag(P–P)_2]NO_3$ with unco-ordinated anion and bidentate phosphine ligands. These complexes have greatly enhanced kinetic and thermodynamic stabilities with respect to similar $AgP_4$ complexes containing monodentate phosphines.

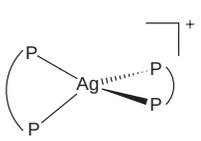


In the present study the evidence from $^{31}P$, $^1H$ and $^{13}C$ NMR spectra (Tables 1–3) is consistent with a similar structural type for 1 : 2 adducts of $AgNO_3$ with d3pype and d4pype. In contrast

**Table 1** Phosphorus-31 and $^{109}$Ag NMR parameters for $\{[Ag(dnpype)_2]^+\}_n$ complexes

| | | | $\delta(^{31}P)$[a] | | | $\delta(^{109}Ag)$[b] | | | $^1J(^{109}Ag–^{31}P)$[c]/Hz | | |
|---|---|---|---|---|---|---|---|---|---|---|---|
| Compound | Solvent | $T$/K | $P_A$ | $P_B$ | $P_C$ | $Ag_X$[d] | $Ag_Y$[d] | $Ag_Z$ | $P_A$ | $P_B$ | $P_C$ |
| $\{[Ag(d2pype)_2]NO_3\}_n$ | $CD_3OD$ | 243 | | | | | | | | | |
| $n = 1$ | | | 7.3 | | | 1411 | | | 266 | | |
| $n = 2$ | | | 3.1 | 12.3 | | | 1417 | | 218[e] | *ca.* 326 | |
| $n = 3$ | | | 1.0 | 15.9 | 6.1 | | 1397 | 1386 | 203[f] | *ca.* 330 | *ca.* 257 |
| $\{[Ag(d2pype)_2]NO_3\}_n$ | | 295 | | | | | | | | | |
| $n = 1$ | | | 7.3 | | | 1400 | | | | | |
| $n = 2$ | | | 3.1 | 12.3 | | | 1395 | | | | |
| $[Ag(d3pype)_2]NO_3$ | $D_2O$ | 295 | −5.5 | | | 1418 | | | 266 | | |
| $[Ag(d4pype)_2]NO_3$ | $CD_3OD$ | 295 | 2.2 | | | 1378 | | | 263 | | |

[a] Referenced to external 85% $H_3PO_4$ at 295 K. [b] Referenced to 4 M $AgNO_3$ in $D_2O$, estimated error in chemical shifts ±5 ppm. [c] ±1 Hz for $P_A$ and ±10 Hz for $P_B$ and $P_C$ signals which are complex second-order multiplets. [d] The $^{109}$Ag chemical shifts of the monomer and dimer have different temperature dependencies: $Ag_X$ −0.21 ppm $K^{-1}$; $Ag_Y$ −0.42 ppm $K^{-1}$. [e] $^2J(P_A–P_B) = 41$ Hz. [f] $^2J(P_A–P_B) = 49$ Hz.

**Table 2** Carbon-13 NMR data for 2-, 3- and 4-pyridyl ligands and silver(I) complexes (at ambient temperature)

| | | $\delta(^{13}C)$,[a] $J$(C–P)/Hz | | | | | |
|---|---|---|---|---|---|---|---|
| Compound | Solvent | $C^2$ | $C^3$ | $C^4$ | $C^5$ | $C^6$ | $CH_2$ |
| d2pype[b] | $CDCl_3$ | 162.3 | 129.1 (vt) (11) | 136.3 | 123.0 | 149.8 | 22.1 |
| $\{[Ag(d2pype)_2]NO_3\}_n$[c] | $CDCl_3$ | 157.4 | 129.2 | 136.1 | 124.1 | 149.8 | 23.0 |
| d3pype | $CDCl_3$ | 153.2 (vt) (12.6) | 132.4 (vt) (9.0) | 139.8 (vt) (7.3) | 123.7 | 150.3 | 22.9 |
| $[Ag(d3pype)_2]NO_3$ | $D_2O$ | 151.5 | 126.8 | 141.1 | 125.2 | 151.2 | 23.5 |
| d4pype | $CDCl_3$ | 149.8 | 126.9 (vt) (8.1) | 146.3 (vt) (9.9) | 126.9 (vt) (8.1) | 149.8 | 22.3 |
| | $CD_3OD$ | 150.2 | 128.9 (vt) (8.5) | *d* | 128.9 (vt) (8.5) | 150.2 | 23.2 |
| $[Ag(d4pype)_2]NO_3$ | $D_2O$ | 150.3 | 127.9 | 141.7 | 127.9 | 150.3 | 24.0 |

[a] Singlet, unless otherwise stated. [b] Assignments based on $^{13}$C assignments for the bidentate 2-pyridylphosphine $Ph(2py)P(CH_2)_2PPh(2py)$.[13] [c] Separate $^{13}$C resonances for monomer ($n = 1$) and dimer ($n = 2$) are not resolved. [d] Not resolved.

**Table 3** Proton NMR data for 2-, 3- and 4-pyridyl ligands and silver(I) complexes (at ambient temperature)

| | | $\delta(^1H)$ | | | | | |
|---|---|---|---|---|---|---|---|
| Compound | Solvent | $H^2$ | $H^3$ | $H^4$ | $H^5$ | $H^6$ | $CH_2$* |
| d2pype | $CD_3OD$ | | 7.43 | 7.69 | 7.29 | 8.56 | 2.44 (8.7) |
| $\{[Ag(d2pype)_2]NO_3\}_n$ | $CD_3OD$ | | | | | | |
| $n = 1$ | | | 7.44 | 7.57 | 7.30 | 8.55 | 2.95 |
| $n = 2$ | | | 7.37 | 7.43 | 7.13 | 8.28 | 3.12 |
| | | | 7.35 | 7.46 | 7.15 | 8.19 | 3.00 |
| d3pype | $CDCl_3$ | 8.59 | | 7.59 | 7.27 | 8.59 | 2.16 (8.7) |
| | $D_2O$ | 8.09 | | 7.18 | 6.90 | 8.09 | 1.81 |
| $[Ag(d3pype)_2]NO_3$ | $D_2O$ | 8.57 | | 7.87 | 7.42 | 8.47 | 2.86 |
| d4pype | $CDCl_3$ | 8.58 | 7.18 | | 7.18 | 8.58 | 2.12 (9.3) |
| | $CD_3OD$ | 8.39 | 7.27 | | 7.27 | 8.39 | 2.19 (9.7) |
| $[Ag(d4pype)_2]NO_3$ | $CD_3OD$ | 8.43 | 7.32 | | 7.32 | 8.43 | 2.77 |

* Broad singlet or quasi-triplet [$J = {}^2J(^{31}P–^1H) + {}^3J(^{31}P–^1H)$ (Hz) in parentheses where resolved].

to the complexes with phenyl-substituted phosphines these complexes are highly soluble in water. The $^{31}$P NMR spectra of both complexes consist of two overlapping doublets (intensity ratio 51:49). The $^1J(^{31}P–^{107,109}Ag)$ spin–spin couplings were resolved at ambient temperature and the values (Table 1) are typical of those expected for bis-chelated complexes with tetrahedral $AgP_4$ co-ordination.[11,12] The $^1$H NMR data (Table 3) are consistent also with the formation of simple monomeric species. For bidentate phosphines with $(CH_2)_2$ backbones (*e.g.* dppe) the $CH_2$ protons constitute the AA′ part of an $A_2XX'A_2'$ spin system as a result of unequal $^{31}P–^1H$ spin–spin coupling to the two P atoms and give rise to a quasi-triplet in which the separation of the outer two peaks corresponds to $|^2J(^{31}P–^1H) + {}^3J(^{31}P–^1H)|$. This pattern is observed for the d*n*pype ligands (Table 3) and the small downfield co-ordination shift (Δδ 0.6–1.0) and broadening of the $(CH_2)_2$ resonance to give an unresolved multiplet is characteristic of the behaviour observed previously for bis-chelated gold(I) diphosphine complexes.[14] For $[Au(dppe)_2]Cl$ the aromatic protons were shielded with respect to those of the free diphosphine but this was not observed here for $[Ag(dnpype)_2]NO_3$ ($n = 3$, 4) where all protons are slightly deshielded (Δδ < 0.1) with respect to d3pype or d4pype (Table 3).

The $^{109}$Ag chemical shifts (Table 1), obtained from [$^{31}$P–$^{109}$Ag] HMQC spectra, lie within the range observed previously[11,15] for $[Ag(dppe)_2]NO_3$ and analogous bis-chelated $AgNO_3$ complexes of bidentate phenylphosphines, where the strong deshielding (high frequency end of the known $^{109}$Ag shift range) was attributed to the good π-acceptor properties of the bidentate phosphine ligands.[11]

In contrast with the above results, the $^{31}$P NMR solution spectra for the 2-pyridyl complex were found to be considerably more complex. Variable-temperature data recorded in $CH_3OH$–$CD_3OD$ solution are shown in Fig. 1 with chemical shift and coupling constant data in Table 1. At 298 K the spectrum consisted of two overlapped doublets [δ 7.3, $^1J(^{107,109}Ag–^{31}P)$ 231, 266 Hz] and two pairs of broadened multiplets at δ 3.1 and 12.3. On cooling the solution the peaks sharpened and the pair

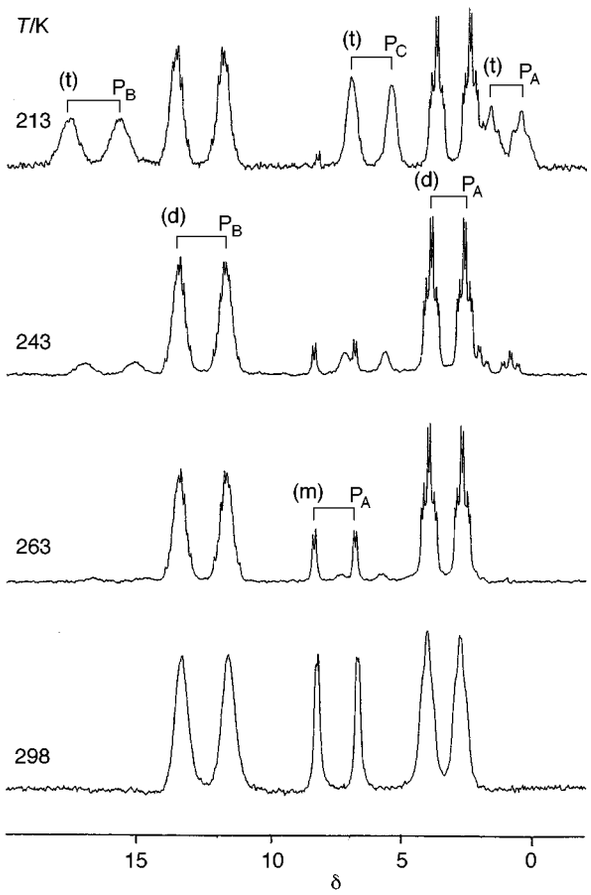


**Fig. 1** 161.9 MHz $^{31}P$-{$^{1}H$} NMR spectra of {[Ag(d2pype)$_2$]$NO_3$}$_n$ in $CH_3OH$–30% $CH_3OD$ at 298, 263, 243 and 213 K. The resonances are assigned to the monomeric (m), dimeric (d) and trimeric (t) species {[Ag(d2pype)$_2$]$^+$}$_n$

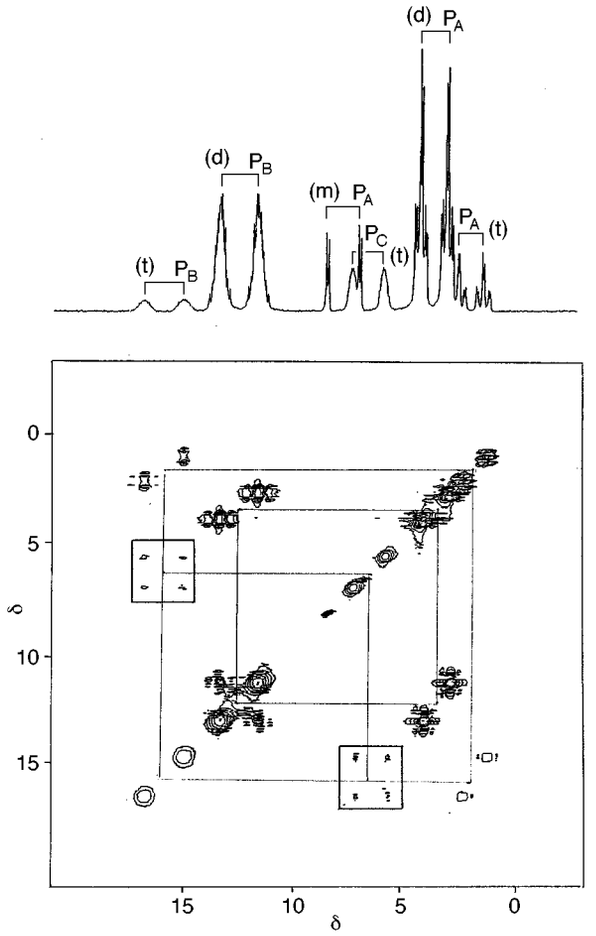


**Fig. 2** Phase-sensitive $^{31}P$-{$^{1}H$} COSY spectrum of the solution of {[Ag(d2pype)$_2$]$NO_3$}$_n$ in $CH_3OH$–30% $CH_3OD$ at 233 K showing connectivities between the $P_A$ and $P_B$ multiplets of the dimer (d) and between the $P_A$ and $P_B$ and $P_B$ and $P_C$ multiplets of the trimer (t). The cross-peaks shown as inserts are plotted at a lower threshold for clarity

of doublets at δ 7.3 gradually decreased in intensity while the other resonances increased in intensity. The fine structure of these multiplets was fully resolved at 263 K where a new set of peaks centred at δ 1.0, 6.1 and 15.9 became visible and increased in intensity with decreasing temperature. As for the 3- and 4-pyridyl complexes, the pair of doublets at δ 7.3, $^{1}J(^{107,109}Ag–^{31}P)$ *ca.* 250 Hz is typical for monomeric tetrahedral bis-chelated [Ag(P–P)$_2$]$^+$ complexes with four equivalent P atoms[11,12] and is accordingly assigned as the monomeric species [Ag(d2pype)$_2$]$^+$.

The multiplets at δ 3.1, 12.3 are assigned, however, to the dimeric complex {[Ag(d2pype)$_2$]}$_2^{2+}$ with both chelating and bridging phosphine ligands. Although each silver(I) ion in this dimer has $AgP_4$ co-ordination, there are two distinct phosphorus environments for chelated ($P_A$) and bridging ($P_B$) d2pype ligands, respectively. The $^{31}P$ COSY spectrum (Fig. 2) shows cross-peaks between the two multiplets confirming that they are part of the same spin system and the assignment is further substantiated by the [$^{31}P$–$^{109}Ag$] HMQC NMR spectrum (Fig. 3) which shows two $^{31}P$–$^{109}Ag$ two-dimensional cross-peaks with identical $^{109}Ag$ chemical shifts (δ 1417), consistent with only one type of silver environment ($Ag_Y$). The high field $^{31}P$ multiplet (δ 3.1) can be assigned to the chelated ($P_A$) environment and the multiplet at δ 12.3 to the bridging ($P_B$) environment, based on the splitting patterns. Although the spin system is second order the $^{5}J(P_A–P_B)$ coupling is expected to be only very small. By recording a $^{109}Ag$-edited $^{31}P$ NMR spectrum

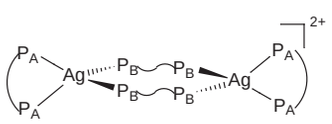


(thus removing transitions associated with the $^{107}Ag$ isotope) the $P_A$ multiplet simplified to a pair of virtual triplets from which the values of $^{1}J(^{31}P_A–^{109}Ag)$ and $^{2}J(P_A–P_B)$ were obtained (Table 1). The $^{2}J(P_A–P_B)$ coupling (41 Hz) corresponds to the coupling of P atoms in the chelated and bridging d2pype ligands across silver and is comparable to that observed for the $^{2}J$[P(Ph$_2$)–Ag–P(Et$_2$)] coupling in the tetrahedral silver(I) complex [Ag{Ph$_2$P(CH$_2$)$_2$PEt$_2$}$_2$]$NO_3$ (50 Hz).[11] The $P_B$ multiplet has a greater complexity, as a consequence of couplings to both Ag atoms, and the spin system is not readily analysable, even in the simplified $^{109}Ag$-edited $^{31}P$ spectrum. However, based on the splitting between the two symmetrical halves of the multiplet, the $^{1}J(^{31}P_B–^{109}Ag)$ coupling is estimated to be *ca.* 326 Hz and *ca.* 50% greater than $^{1}J(^{31}P_A–^{109}Ag)$, despite only small differences in the values of the Ag–P bond distances found in the crystal structure (see below). The equilibrium between the monomer and dimer can be represented by equation (1), with equilibrium

$$[Ag(d2pype)_2] + [Ag(d2pype)_2] \rightleftharpoons [\{Ag(d2pype)_2\}_2] \quad (1)$$

constant $K_1 = [\{Ag(d2pype)_2\}_2]/[Ag(d2pype)_2]^2$. The relative concentrations of monomer and dimer were determined by comparison of the $^{31}P$ peak integrals for a solution of [Ag(d2pype)$_2$]$^+$ in $CD_3OD$ (5.0 mM based on [Ag]$^+$).§ Values of $K_1$ were obtained in the temperature range 298–213 K and are presented in Table 4. A plot of ln $K_1$ *vs.* $1/T$ gives $R^2 = 0.98$

§ At this concentration the complex remained totally soluble in the temperature range 298 to 213 K.

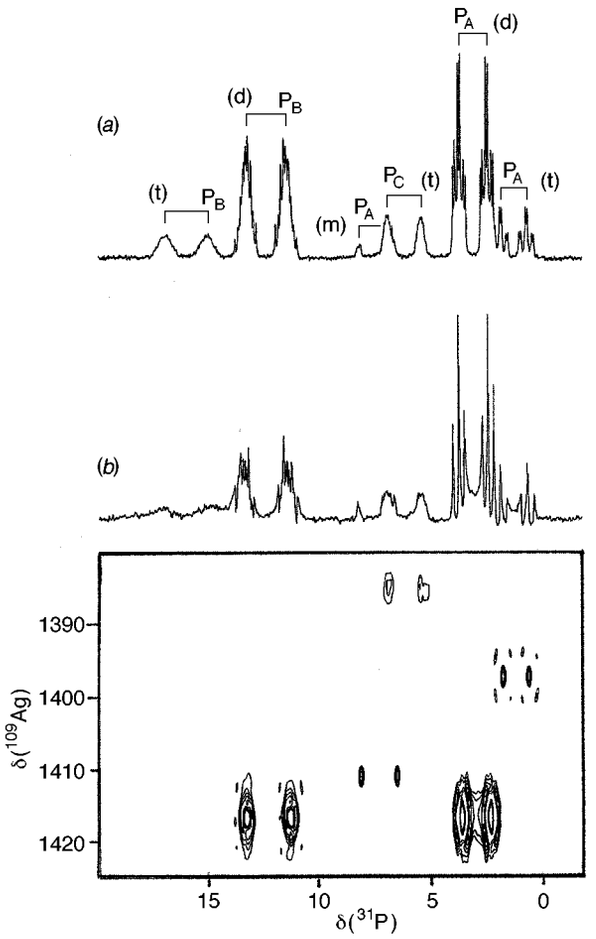


**Fig. 3** The normal $^{31}P$ NMR spectrum of a solution of $\{[Ag(d2pype)_2]NO_3\}_n$ at 243 K (*a*), and the [$^{31}P$–$^{109}Ag$] HMQC NMR spectrum in $CD_3OD$ at the same temperature (*b*)

**Table 4** Values of ln $K_1$ and ln $K_2$ as a function of temperature for $\{[Ag(d2pype)_2]^+\}_n$ for total $[Ag^+] = 5.0 \times 10^{-3}$ mol $l^{-1}$ in $CH_3OH$–$CD_3OD$ solution

| *T*/K | $10^3$ [monomer]/ mol $l^{-1}$ | $10^3$ [dimer]/ mol $l^{-1}$ | $10^3$ [trimer]/ mol $l^{-1}$ | ln $K_1$ | ln $K_2$ |
|---|---|---|---|---|---|
| 295 | 1.16 | 1.92 | 0.00 | 7.26 | — |
| 283 | 0.83 | 2.09 | 0.00 | 8.02 | — |
| 273 | 0.60 | 2.15 | 0.03 | 8.69 | 3.14 |
| 263 | 0.43 | 2.19 | 0.06 | 9.38 | 4.15 |
| 253 | 0.32 | 2.12 | 0.14 | 9.94 | 5.33 |
| 243 | 0.19 | 1.97 | 0.29 | 10.91 | 6.65 |
| 233 | 0.085 | 1.77 | 0.46 | 12.38 | 8.01 |
| 223 | 0.095 | 1.66 | 0.53 | 12.12 | 8.12 |
| 213 | 0.04 | 1.67 | 0.54 | 13.86 | 9.00 |

for ln $K_1 = (4893/T) - 9.232$ (Fig. 4), yielding values for $\Delta H^\circ$ and $\Delta S^\circ$ of −41 (±2) kJ $mol^{-1}$ and −77 (±5) J $K^{-1}$ $mol^{-1}$, respectively.

The peaks at δ 1.0, 6.1 and 15.9 which first appear in the spectrum at 263 K are assigned to formation of a trimeric cluster $[\{Ag(d2pype)_2\}_3]^{3+}$ which has three non-equivalent phosphorus sites and two non-equivalent silver sites. In this cluster the terminal chelated ($P_A$) environment would be expected to be similar to that found in the dimer and the high field multiplet (δ 10) has a similar splitting but shifted slightly to low frequency of that of the dimer $P_A$ multiplet at δ 3.1. The values of

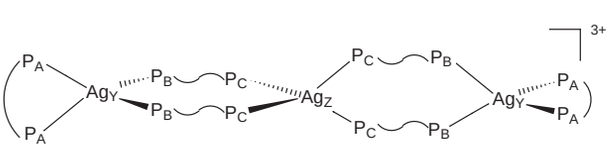


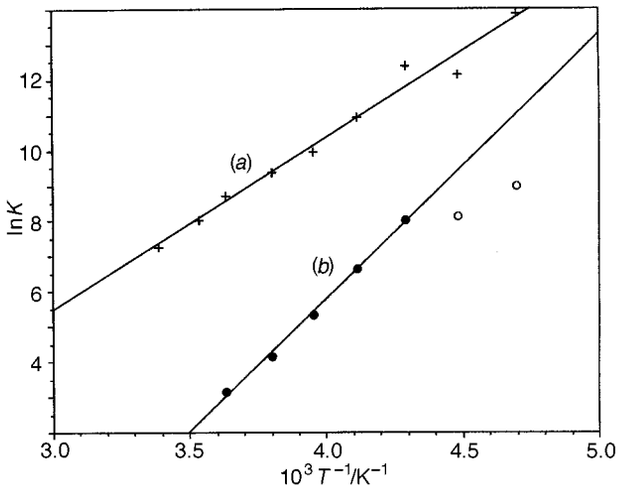


**Fig. 4** Plots of ln $K_1$ (*a*) and ln $K_2$ (*b*) *vs.* $1/T$ for the equilibria obtained from variable-temperature $^{31}P$ NMR spectra of a solution of $\{[Ag(d2pype)_2]NO_3\}_n$ in $CD_3OD$ (5.0 mM based on $[Ag^+]$)

$^1J(^{31}P_A$–$^{109}Ag)$ 203 Hz and $^2J(P_A$–$P_B)$ 49 Hz, obtained from the $^{109}Ag$-edited $^{31}P$ spectrum, are slightly lower and higher, respectively, than for the dimer, suggesting a relative weakening of Ag–P bond strength in the chelate and a strengthening of the Ag–P (bridging) bonds with respect to the analogous environment of the dimer. The trimer also has two non-equivalent phosphorus environments for bridging d2pype ligands ($P_B$ and $P_C$) co-ordinated to the terminal and central Ag atoms, respectively. The broadened multiplet at δ 15.9 is assignable to $P_B$, based on the chemical shift (which is closest to that of the $P_B$ multiplet of the dimer) and the $^1J(^{109}Ag$–$^{31}P_B)$ coupling, estimated to be *ca.* 330 Hz based on the splitting between the two symmetrical halves of the multiplet in the $^{109}Ag$-edited $^{31}P$ spectrum, which is similar to that of the dimer. The broadened doublet at δ 6.1 is assigned to $P_C$ and has similar chemical shift and $^1J(^{109}Ag$–$^{31}P)$ coupling (*ca.* 257 Hz) to that of the monomer. These assignments are substantiated by the $^{31}P$ COSY spectrum of the solution at 233 K (Fig. 2) which shows the expected cross-peaks between the $P_A$ and $P_B$ multiplets and a second set of cross-peaks between the $P_B$ and $P_C$ multiplets. No correlation is observed between $P_A$ and $P_C$ which would require a resolved $^5J$(P–P) coupling. The trimer contains non-equivalent silver environments for the terminal ($Ag_Y$) and central ($Ag_Z$) silver atoms and therefore two distinct $^{109}Ag$ chemical shifts are expected in the $^{109}Ag$ NMR spectrum. These are clearly visible in the [$^{31}P$–$^{109}Ag$] HMQC spectrum at 243 K (Fig. 3) with $^{31}P/^{109}Ag$ cross-peaks for Ag–$P_A$ at δ 1.0/1397 and Ag–$P_C$ at δ 6.1/1386. A peak for Ag–$P_B$ (expected at 15.9/1397) is not resolved in Fig. 3 presumably because the $^{31}P_B$ multiplet is very broad and signal intensity is lost due to relaxation during the HMQC pulse sequence.

The equilibrium between the monomer, dimer and trimer is represented by equation (2) with $K_2 = [\{Ag(d2pype)_2\}_3]/[\{Ag(d2pype)_2\}_2][Ag(d2pype)_2]$. As for the monomer–dimer

$$[\{Ag(d2pype)_2\}_2] + [Ag(d2pype)_2] \rightleftharpoons [\{Ag(d2pype)_2\}_3] \quad (2)$$

equilibrium, the relative concentrations of the three species are obtainable directly from peak integrals yielding values of $K_2$ as a function of temperature (Table 4). The plot of ln $K_2$ *vs.* $1/T$ in the temperature range 233–263 K (Fig. 4) gives $R^2 = 0.99$ for ln $K_2 = 7504(1/T) - 24.26$ and yields values of $\Delta H^\circ$ and $\Delta S^\circ$ of −62 (±2) kJ $mol^{-1}$ and −200 (±5) J $K^{-1}$ $mol^{-1}$ respectively. Values of $K_2$ determined at 213 and 223 K are significantly lower than predicted and while both broadening and overlap of peaks makes the estimation of $K_2$ at these temperatures less

meaningful the possibility of further aggregation to tetrameric or higher order clusters cannot be discounted. Such clusters would contain a greater number of $P_C$ phosphorus sites relative to $P_A$ and $P_B$ with chemical shifts that would be expected to be similar to and overlap with those of the trimer which would result in a greater intensity of the $P_C$ multiplet relative to $P_A$ and $P_B$. The observation of a small increase in the relative intensity at 213 K for the $P_C$ multiplet is consistent with this.

As for the 3- and 4-pyridyl complexes, the $^{109}$Ag chemical shifts for $\{[Ag(d2pype)_2]^+\}_n$ occur within the range observed previously for $AgP_4$ complexes of phenyl-substituted diphosphines.[11,15] The $^{109}$Ag chemical shifts become more shielded with increase in temperature, but the $^{109}$Ag environments in the monomer and dimer exhibit different temperature dependencies (Table 1) so that at 295 K the $^{109}$Ag shift of the dimer is to lower frequency of the monomer, but this situation is reversed at 243 K. For the trimer the $^{109}$Ag shifts of both Ag are significantly more shielded than those of the dimer at the same temperature.

The presence of an equilibrium mixture of the monomeric and dimeric d2pype species in methanol was not apparent in $^{13}$C NMR spectra, because separate peaks for monomer and dimer were not resolved (Table 2), but it was evident in the variable-temperature $^1$H NMR spectra of the system, albeit less easily followed than in the $^{31}$P spectra due to considerable overlap of resonances. However, in the aromatic region the H$^6$ proton of the pyridine ring of 2-pyridylphosphines is strongly deshielded from the remaining aromatic protons[16] and occurs in a clear region of the spectrum. At 298 K all $^1$H resonances were broadened but multiplet splitting patterns were resolved on cooling to 273 K. For the monomer the H$^6$ resonance could be assigned to a peak at δ 8.55 since this decreased in intensity on cooling the solution, consistent with the behaviour observed in the $^{31}$P NMR spectra. Similarly a pair of peaks of equal intensity at δ 8.19 and 8.28 could be assigned to the H$^6$ protons of pyridyl rings in the dimer in non-equivalent chelated and bridged d2pype ligands. By using these resonances as a reference point the other pyridyl $^1$H resonances of the monomer and dimer could be assigned from observed connectivities in phase-sensitive double-quantum filtered $^1$H COSY spectra. These assignments are in Table 3. Additional resonances appeared in the aromatic region as the solution was cooled which are possibly due to the trimer, but the peaks were too broad to allow a complete assignment.

The $^{31}$P NMR spectra recorded at 295 K for solutions of $\{[Ag(d2pype)_2]NO_3\}_n$ of equal concentration (10.2 mM based on $[Ag^+]$) in a range of solvents show the relative percentages of the monomer and dimer to be strongly solvent dependent with the concentration of the monomer decreasing from *ca.* 67% in $CHCl_3$ and $CH_2Cl_2$ to 19% in methanol and 12% in ethanol, while in acetonitrile the dimer was found to be the only species present in the solution with no signal from the monomeric species observed. These data suggest that the $[M(P–P)_2]^+$ cations in these systems are not isolated species in solution but interact strongly with solvent such that equilibrium (1) is likely to be more properly represented by equation (1a) or similar

$$2[M(P–P)_2]^+X^-.solv \rightleftharpoons [\{M(P–P)_2\}_2]^{2+}2X^-.solv \quad (1a)$$

with involvement of anion as well as solvent. Within this context, the relative stability of the monomeric, dimeric and trimeric species will depend not only on the relative stabilities of the isolated cations, but also on differences in the strength of intermolecular interactions between the anion, solvent and cation. While a detailed analysis of the reasons as to underlying cause(s) for the shift of the equilibrium to the left for complexes with dppe, d3pype and d4pype ligands and to the right for d2pype requires the collection of further spectroscopic and structural data on complexes with a variety of counter anions in a wider range of solvents, it is clear from the present results that the position of the pyridine nitrogen in the ring has a significant effect on this chemistry.

The mechanism of the transition between the monomeric, dimeric and trimeric 2-pyridyl species requires the breaking of at least one Ag–P bond for each silver atom and, in principle, formation of unco-ordinated P atoms. We have shown previously that this mechanism occurs for 1:2 adducts of silver(I) salts with 1,3-bis(diphenylphosphino)propane (dppp), where there is an equilibrium in solution between neutral [AgX(dppp-*P*,*P*′)(dppp-*P*)] and ionic [Ag(dppp-*P*,*P*′)$_2$]X, with the position of the equilibrium dependent on the nature of the anion, X.[12] In the present case there is no evidence from the $^{31}$P NMR spectra for unco-ordinated P, which suggests that the process may involve formation of clusters of monomers, for example of the type $\{[M(P–P)_2]^+X^-[M(P–P)_2]^+\}$ (observed as minor species in the electrospray mass spectrum) which are then able to rearrange in a concerted fashion to form dimeric or higher order complexes at a rate faster than the NMR timescale.

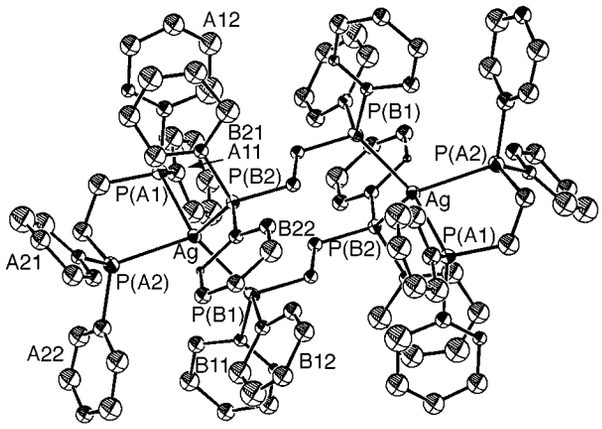


**Fig. 5** Representative view of the $[Ag_2(d2pype)_4]^{2+}$ cation of $[Ag_2(d2pype)_4][NO_3]_2·2CH_2Cl_2$

**Table 5** Geometric parameters (bond lengths in Å, angles in °) for dimeric complexes

| | Ag/d2pype[a] | Ag/dppe[b] | Ag/dmpe[c] | Cu/dmpe[d] |
|---|---|---|---|---|
| M–P(A1) | 2.50(1) | 2.597 | 2.557(6) | 2.289(1) |
| M–P(A2) | 2.521(8) | 2.509 | 2.491(4) | 2.293(1) |
| M–P(B1) | 2.46(1) | 2.526 | 2.471(4) | 2.267(1) |
| M–P(B2) | 2.496(8) | 2.550 | 2.465(4) | 2.263(1) |
| Average M–P | 2.49(3) | 2.55(4) | 2.50(4) | 2.28(2) |
| P(A1)–Ag–P(A2) | 83.4(3) | 84.1 | 83.5(2) | 89.2(1) |
| P(A1)–Ag–P(B1) | 125.5(3) | 118.0 | 114.1(2) | 116.9(1) |
| P(A1)–Ag–P(B2) | 110.3(3) | 119.4 | 144.4(2) | 113.2(1) |
| P(A2)–Ag–P(B1) | 115.1(3) | 118.5 | 115.6(2) | 110.3(1) |
| P(A2)–Ag–P(B2) | 120.7(3) | 106.4 | 117.6(2) | 115.1(1) |
| P(B1)–Ag–P(B2) | 102.6(3) | 108.4 | 109.6(2) | 110.7(1) |

[a] This work. [b] Ref. 17. [c] Ref. 19. [d] Ref. 18.

## Crystal structure

The results of the room-temperature single-crystal X-ray study on crystals obtained from recrystallization of the 1:2 adduct of $AgNO_3$ with d2pype from $CH_2Cl_2$–$Et_2O$ solution are consistent with the formation of dimeric cations, $[(d2pype)Ag(\mu\text{-}d2pype)_2Ag(d2pype)]^{2+}$, unco-ordinated nitrate anions and solvated dichloromethane. Importantly, this complex is isomorphous with the methanol solvate of the analogous dppe complex.[17] A projection of the cation is shown in Fig. 5 with relevant geometric parameters for the two structures listed in Table 5. The two halves of the cation dimer are related by a centre of crystallographic symmetry with each silver atom co-ordinated

to one bidentate and two bridging d2pype ligands with the bridging ligands and silver atoms forming a ten-membered ring in a double boat conformation.

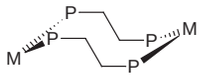


This structural type is rare for Group 11 bidentate phosphine complexes, being recorded previously only for $[Ag(dppe)_2]_2[NO_3]_2$[17] and for $[Cu(dmpe)_2][BF_4]_2$[18] and $[Ag(dmpe)_2]_2[BPh_4]_2$,[19] the majority of reported structures existing as the tetrahedral monomer[12,20] or, for copper complexes, as 2:3 dimers with co-ordinated anion, X, displacing the second bridging phosphine.[21–26] However, X-ray crystallographic studies currently in progress show that 1:2 complexes of gold chloride[27] and copper iodide[28] with d2pype also crystallize as solvated dimers analogous to the present silver nitrate complex, suggesting that the dimeric structural type may be stabilized in the solid state with respect to the monomer by the d2pype ligand.

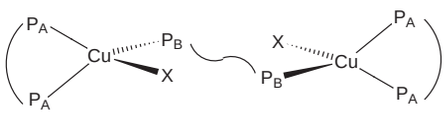


In the present structure the pyridyl groups on the chelating and bridging ligands adopt both approximate edge-face and butterfly wing conformations with acute Ag–P–$C_{ipso}$–$C_{ortho}$ torsion angles of 16.8, 74.7° [P(A1)], −63.5, 65.8 [P(A2)], −1.1, −82.2 [P(B1)] and −54.9, 28.3° [P(B2)]. The bridging pyridyl substituents occupy approximately axial and equatorial positions in the ten-membered ring with the axial groups from adjacent ligands atoms adopting a face-face conformation (Fig. 5). The nitrate group is located in a general lattice position adjacent to the chelating phosphine and forms a weak hydrogen bond with the solvated $CH_2Cl_2$ (O · · · H *ca.* 2.4 Å). The $CH_2Cl_2$ molecule lies in proximity to three phenyl rings: (A11), (A22) from the chelating ligand and (B11) from the bridging ligand. The Ag–P bond lengths range from 2.46(1) to 2.521(8) Å with an average value of 2.49(3) Å (Table 5). The two Ag–$P_A$ distances are marginally shorter than the Ag–$P_B$ distances, but probably not significantly so given the relatively poor quality of the X-ray data. For comparison, the average values of Ag–P for the analogous dppe and dmpe complexes are 2.55(4) and 2.50(4) Å respectively, while values for the monomeric tetrahedral complexes $[Ag(dppe)_2]NO_3$[20] and $[Ag(dppp)_2]SCN$[12] are 2.52(2) and 2.52(1) Å. Overall, the changes in substituent or co-ordination mode from chelating to bridging appear to have only a marginal effect on the Ag–P bond lengths. The P–Ag–P angles reflect differences in chelate *versus* bridging co-ordination with $P_B$–Ag–$P_B$ 102.6(3)° greater than $P_A$–Ag–$P_A$ 83.4(3)° while the four $P_A$–Ag–$P_B$ angles are each greater than the tetrahedral angle, ranging from 110.3(3) to 125.5(3)°.

Finally, we note that the results of this work provide no evidence for the co-ordination of the pyridyl N atoms (either in the solid state or in solution). Previous work on diphenyl(2-pyridyl)phosphine complexes $[PPh_2(2py)]$ with silver chloride have shown that for the dimeric system $[\{PPh_2(2py)\}Ag(\mu\text{-}Cl)_2\{\mu\text{-}PPh_2(2py)\}Ag\{PPh_2(2py)\}]$ the two silver atoms have $AgCl_2P_2$ and $AgCl_2PN$ co-ordination with one of the $PPh_2(2py)$ ligands bridging the two Ag atoms in a P, N bidentate fashion,[29] while for the tetrameric complex $[\{Ag[PPh_2(2py)]Cl\}_4]$ no nitrogen co-ordination occurs,[30] with the conclusion that pyridine N-co-ordination to silver is only possible when chloro/phosphorus co-ordination is not sufficient for co-ordinative saturation. It was proposed also[30] that weak donor atoms such as $BF_4^-$ or $PF_6^-$ would favour N-co-ordination. In the present case with the nitrate anion, however, this is prevented by the apparent strong preference of the silver for the $AgP_4$ co-ordination sites through either chelation or bridging co-ordination of the diphosphine ligands.

## Conclusion

The 1:2 complexes $AgNO_3$ with bidentate pyridylphosphine ligands are more hydrophilic than the phenyl-substituted analogues and the degree of hydrophilicity depends critically on the position of the pyridyl N atom. The results presented here are of importance to the interpretation of the antitumour properties of complexes of this type. We have shown here that the association equilibrium between the monomeric and dimeric forms of $\{[Ag(d2pype)_2]^+\}_n$ is solvent dependent and we have reported elsewhere[3] that $^{31}P$ NMR signals assignable to both the monomeric and dimeric species were observed for $\{[Ag(d2pype)_2]^+\}_n$ in blood plasma at 37 °C. Clearly such an association equilibrium must be taken into account when considering the likely speciation of the complex *in vivo*. The structural results for $[\{Ag(d2pype)(\mu\text{-}d2pype)\}_2][NO_3]_2$ show that the solvent is incorporated within the lattice and the 2-pyridyl complex has only limited solubility in water. The location of the pyridyl N atom within the inner core of the cation means that the lipophilic properties of the 2-pyridyl complexes are not likely to vary greatly between the various species. On the other hand, the increased hydrophilic character of the monomeric 3-pyridyl and 4-pyridyl complexes is a consequence of the more exposed N atoms. Several classes of lipophilic cations with antimitochondrial antitumour activity have demonstrated a relationship between antitumour selectivity and lipophilic–hydrophilic balance and our preliminary studies show a similar relationship for these silver(I) complexes and for related gold(I) pyridylphosphine complexes, when tested against human ovarian cancer cell lines in culture.[8] We are currently investigating further the antitumour selectivity of these types of complexes.

## Acknowledgements

We acknowledge support of this work by the Australian Research Council and the Australian National Health & Medical Research Council (R. Douglas Wright Award to S. J. B.-P.) and thank Dr. Rodney Sue for assistance with some of the NMR experiments and Dr. Paul Bowyer, Research School of Chemistry, Australian National University, for recording the electrospray mass spectra. We are grateful also to Associate Professor Allan White, Dr. Brian Skelton and Dr. Effendy and the University of Western Australia Crystallographic Centre for recollection of the structural data for $[\{Ag(d2pype)_2\}_2][NO_3]_2$ and expert advice and assistance in the structure determination and thank Dr. Ken Busfield for helpful advice on the thermodynamic data.

## References

1 S. J. Berners-Price and P. J. Sadler, *Struct. Bonding* (*Berlin*), 1988, **70**, 27.
2 S. J. Berners-Price, R. K. Johnson, A. J. Giovenella, L. F. Faucette, C. K. Mirabelli and P. J. Sadler, *J. Inorg. Biochem.*, 1988, **33**, 285.
3 S. J. Berners-Price and P. J. Sadler, *Coord. Chem. Rev.*, 1996, **151**, 1.
4 Y. Dong, S. J. Berners-Price, D. R. Thorburn, T. Antalis, J. Dickinson, T. Hurst, L. Qui, S. K. Khoo and P. G. Parsons, *Biochem. Pharmacol.*, 1997, **53**, 1673.
5 S. J. Berners-Price, D. C. Collier, M. A. Mazid, P. J. Sadler, R. E. Sue and D. Wilkie, *Metal-Based Drugs*, 1995, **2**, 111.
6 W. A. Denny, G. J. Atwell, B. C. Baguley and B. F. Cain, *J. Med. Chem.*, 1979, **22**, 134.
7 D. C. Rideout, T. Calogeropoulou, J. S. Jaworski, R. J. Dagino and M. R. McCarthy, *Anti-Cancer Drug Design*, 1989, **4**, 265.
8 S. J. Berners-Price, R. J. Bowen, M. J. McKeage, P. Galettis, L. Ding, C. Baguley and W. Brouwer, *J. Inorg. Biochem.*, 1997, **67**, 154.

9 R. J. Bowen, A. C. Garner, S. J. Berners-Price, I. D. Jenkins and R. E. Sue, *J. Organomet. Chem.*, in the press.
10 S. R. Hall, H. D. Flack and J. M. Stewart, *The XTAL 3.2 Reference Manual*, Universities of Western Australia, Geneva and Maryland, 1992.
11 S. J. Berners-Price, C. Brevard, A. Pagelot and P. J. Sadler, *Inorg. Chem.*, 1985, **24**, 4278.
12 D. Affandi, S. J. Berners-Price, Effendy, P. J. Harvey, P. C. Healy, B. E. Ruch and A. H. White, *J. Chem. Soc.*, *Dalton Trans.*, 1997, 1411.
13 P. H. M. Budzelaar, J. H. G. Frijns and A. G. Orpen, *Organometallics*, 1990, **9**, 1222.
14 S. J. Berners-Price and P. J. Sadler, *Inorg. Chem.*, 1986, **25**, 3822.
15 S. J. Berners-Price, P. J. Sadler and C. Brevard, *Magn. Reson. Chem.*, 1990, **28**, 145.
16 G. E. Griffin and W. A. Thomas, *J. Chem. Soc. B*, 1970, 477.
17 H. Yang, L. Zheng, Y. Xu and Q. Zhang, *Wuji Huaxue Xuebao*, 1992, **8**, 65 (*Chem. Abstr.*, 1992, 117 212 593e).
18 B. Mohr, E. E. Brooks, N. Rath and E. Deutsch, *Inorg. Chem.*, 1991, **30**, 4541.
19 V. Saboonchian, G. Wilkinson, B. Hussain-Bates and M. B. Hursthouse, *Polyhedron*, 1991, **10**, 737.
20 C. S. W. Harker and E. R. T. Tiekink, *J. Coord. Chem.*, 1990, **21**, 287.
21 A. P. Gaughan, R. F. Ziolo and Z. Dori, *Inorg. Chem.*, 1971, **10**, 2776.
22 V. G. Albano, P. L. Bellon and G. Ciani, *J. Chem. Soc.*, *Dalton Trans.*, 1972, 1938.
23 P. Fiaschi, C. Floriani, M. Pasquali, A. Chiesi-Villa and C. Guastini, *Inorg. Chem.*, 1986, **25**, 462.
24 E. W. Ainscough, E. N. Baker, A. G. Bingham, A. M. Brodie and C. A. Smith, *J. Chem. Soc.*, *Dalton Trans.*, 1989, 2167.
25 A. P. Gaughan, K. S. Bowman and Z. Dori, *Inorg. Chem.*, 1972, **11**, 601.
26 E. W. Ainscough, E. N. Baker, M. L. Brader, A. M. Brodie, S. L. Ingham, J. M. Walters, J. V. Hanna and P. C. Healy, *J. Chem. Soc.*, *Dalton Trans.*, 1991, 1243.
27 S. J. Berners-Price, R. J. Bowen, T. W. Hambley and P. C. Healy, unpublished work.
28 S. J. Berners-Price, R. J. Bowen and P. C. Healy, unpublished work.
29 N. W. Alcock, P. Moore, P. A. Lampe and K. F. Mok, *J. Chem. Soc.*, *Dalton Trans.*, 1982, 207.
30 Y. Inoguchi, B. Milewski-Mahrla, D. Neugebauer, P. G. Jones and H. Schmidbaur, *Chem. Ber.*, 1983, **116**, 1487.

*Received* 19*th December* 1997; *Paper* 7/09098F